RAPID ACTIVATION PRODUCT SEPARATIONS FROM FISSION PRODUCTS AND SOIL MATRIXES

Names of the authors: Kevin T. Bennett,[1] Stosh A. Kozimor,[1] Benjamin T. Manard,[2] Veronika Mocko,[1] Susan D. Pacheco,[1] Ann R. Schake,[1] Ruilian Wu,[1] Angela C. Olson[1]*

Title: Rapid Activation Product Separations from Fission Products and Soil Matrixes

Affiliation and address of the authors: [1]Los Alamos National Laboratory, P.O. Box 1663, Los Alamos, NM, 87545, United States; [2]Oak Ridge National Laboratory, 1 Bethel Valley Rd, Oak Ridge, TN, 37830.

Email address of the corresponding author: aolson@lanl.gov

LA-UR-18-31763

RAPID ACTIVATION PRODUCT SEPARATIONS FROM FISSION PRODUCTS AND SOIL MATRIXES

Kevin T. Bennett,[1] Stosh A. Kozimor,[1] Benjamin T. Manard,[2] Veronika Mocko,[1] Susan D. Pacheco,[1] Ann R. Schake,[1] Ruilian Wu,[1] Angela C. Olson[1]*

[1]Los Alamos National Laboratory, P.O. Box 1663, Los Alamos, NM, 87545, United States
[2]Oak Ridge National Laboratory, 1 Bethel Valley Rd., Oak Ridge, TN, 37830, United States

*To whom correspondence should be directed.
e-mail; aolson@lanl.gov
LA-UR-18-31763

Abstract

A rapid method for the separation and qualitative analysis of several neutron activation products (^{198}Au, ^{192}Ir, ^{72}Ga, ^{51}Cr, $^{191/195m/197}$Pt, ^{54}Mn, ^{57}Co, and ^{59}Fe) from fission products and soil matrixes has been developed. Analytes were isolated within 20 h using ion exchange chromatography. After separation, the activation products were characterized by γ-spectroscopy and inductively coupled plasma -optical emission spectroscopy (ICP-OES). Validation experiments demonstrated versatility of the method, showing that the activation products could be isolated from fresh fission products and other contaminants associated with complex soil matrixes.

Keywords

activation products; fission products; rapid separation

Introduction

Advancing environmental fate-and-transport models for non-actinide activation products – those generated from reactions like (n,γ), (n,xn), (n,p), etc. – released from nuclear testing,

radiochemical processing, the storage of nuclear material, and from nuclear power facilities is of widespread interest for accurately evaluating health risks from nuclear contamination sites.[1, 2, 11–16, 3–10] Although substantial efforts have been invested historically to characterize impacts of long-lived activation products ($t_{½}$ > 5 y; ^{60}Co, ^{94}Nb, ^{106m}Ag, ^{63}Ni, ^{99}Tc, ^{93}Mo, $^{152/154}$Eu, etc.),[17] relatively little information is available for activation products that have rapid decay rates ($t_{½}$ < 5 y; ^{51}Cr, ^{54}Mn, ^{57}Co, ^{59}Fe, ^{72}Ga, $^{192/194}$Ir, $^{191/195m/197}$Pt, ^{198}Au, among others).[18–26]

The information reported on short-lived activation products is scarce in comparison to data available for fission products and actinides.[27, 28, 37–39, 29–36] This lack in information has created a clear knowledge gap, and nuclear signatures based on inter-element ratios for non-actinide activation products have yet to be established. This issue can be largely attributed to limited accessibility. For instance, production of many short-lived activation products requires high-energy neutrons (14 MeV), which limits access and impedes efforts to develop separation processes and spectroscopic methods for isotope quantification. The short half-lives also present technical barriers, in that information for short-lived activation product isotopes is often lost for fresh samples – those close in time to a fission event – because fission product and actinide isotopic quantification is prioritized. As demonstrated graphically in Fig. 1, some of these shorter-lived activation product isotopes decay away and are unavailable for detection after a timescale of tens of days or less. Overcoming these obstacles has potential for dramatic impact. For example, making non-actinide activation product quantification more accessible could transition this area of research from an academic curiosity into an analytical tool used broadly to inform policies in global health and national security.

Herein, we describe the first in a series of studies focused on overcoming non-actinide activation product analyses obstacles. We contribute a screening method that removes activation products from fission products and actinides. The procedure avoids complicated and lengthy chromatographic separation schemes[40] and was validated against sample matrixes that contained microscopic quantities of activation products (10^{-3} to 10^{-6} atoms per ^{235}U fission), soil matrixes (90 mg: Standard Reference Material (SRM) 2702), and large quantities of fissioned ^{235}U (up to 80 mg). We observed that precious metals (^{198}Au, $^{192/194}Ir$, $^{191/195m/197}Pt$), main group elements (^{72}Ga), and first row transition metals (^{51}Cr, ^{54}Mn, ^{57}Co, and ^{59}Fe) could be separated from fission products and uranium rapidly for qualitative analysis using gamma spectroscopy (within 20 h). The results are discussed in terms of potential application and future utility for the rapid and qualitative separation method.

Experimental

General Procedure for Separation of Activation Product Elements from Fission Product Elements, Uranium, and Soil Matrix

Two stable carrier solutions are prepared, one containing activation product elements (Au, Co, Cr, Cu, Fe, Ga, Ir, Mn, Ni, Pt, Sc, and Zn at final concentrations of ~0.2 $mg \cdot mL^{-1}$ each, and Pb at ~1 $mg \cdot mL^{-1}$), and the other containing fission product elements and uranium (Ba, Ce, La, Mo, Nd, Sr, Te, Y, Zr, and U at final concentrations of ~0.1 $mg \cdot mL^{-1}$ each). Each solution is generated by combining individual inductively coupled plasma (ICP) standard solutions (SPEX CertiPrep), followed by a matrix transposition to 4 M HNO_3 (Fisher Scientific, Trace Metal Grade). For this study, a National Institute of Standards and Technologies (NIST) SRM 2702 was utilized as a soil standard as it is certified for several activation product analytes employed in this study. As such,

the values can be used to make inductively coupled plasma optical emission spectroscopy (ICP-OES) chemical yielding corrections. Optima-grade (Fisher Scientific) acids (HCl, HNO_3, $HClO_4$, and HF) were used to dissolve 9.99 g of the soil standard following a previously reported standard protocol[41] to generate a 4 M HNO_3 solution with a concentration of ~8.9 mg soil·g^{-1} solution.

The sample matrix solution is prepared by combining 5 mL of the activation product solution, 2 mL of the fission product/U solution, and 10 mL of soil solution (Fig. 2). Precipitation of W is completed by the addition of 1 mL of W carrier solution (SPEX CertiPrep, 10,000 μg·mL^{-1} in H_2O). Following centrifugation, the supernate is removed to yield a W pellet. To the supernate, 0.5 mL of Pb carrier solution is added (SPEX CertiPrep, 10,000 μg·mL^{-1} in 5% HNO_3), followed by 30 mL of fuming HNO_3, then the solution cooled in an ice bath for 1 h to yield a Pb precipitate. The mixture is centrifuged and the supernate removed to yield a Pb pellet, then the solution matrix is converted to 6 M HCl (10 mL). Using a corrosion-resistant Eldex Model 1SIP High Pressure Liquid Metering Pump, the solution is loaded onto a pre-prepared AGMP-1M column (25 mL of resin, 50-100 mesh, in a 40 cm x 6.6 mm Omnifit column). Thirty-seven individual fractions (10 mL each) are collected using a flow rate of 5 mL·min^{-1}. Elution conditions are as follows: 6 M HCl (9 x 10 mL) to elute Mn/Cr/Sc/Ni, Pb/Co (Cut I),[1] and Ir/Cu (Cut II); 4 M HCl (7 x 10 mL); 2 M HCl (8 x 10 mL) to elute Ga/Fe (Cut III); H_2O (4 x 10 mL) to remove Zn (Cut IV); 1% (w/w) thiourea (3 x 10 mL) for the elution of Au (Cut V), and 7% (w/w) thiourea (6 x 10 mL) to recover Pt (Cut VI). For each fraction collected, ICP-OES analysis is performed to determine chemical yields. A representative separation profile showing the percent recovery of the activation products

[1] If Pb does not completely precipitate during the Pb precipitation step, it co-elutes with Co.

and cumulative analyte recovery vs fraction is presented in Fig. 3. Typical percent recoveries achieved for each element over the entire separation are summarized in Table 1.

Guided by the ICP-OES results, the first three fractions are combined and reduced in volume (to 5 mL) to generate the Mn/Ni/Cr/Sc cut, which undergoes further separation on DGA resin (Eichrom; 3 mL of resin in a 20 mL Bio-Rad Econo-Pac column) in order to further remove lanthanide and Groups 2/3/4 fission product elements (e.g. Ba, La, Ce, Sr, Nd, Y, Zr). The DGA-based separation includes an initial load of 5 mL in 6 M HCl, followed by 6 M HCl (2 x 5 mL) to yield Cr/Ni and partially elute Mn; 4 M HCl (2 x 5 mL) to complete elution of Mn; and 2 M HCl (2 x 5 mL) followed by H_2O (2 x 5 mL) to recover Sc. The resultant Cr/Ni, Mn, and Sc fractions are analyzed by ICP-OES to determine chemical yields (Table 1). Typical results achieved from the DGA separation step are illustrated in Fig. 4.

Target Irradiations and Sample Preparation

To generate fresh activation products and fission products, two concurrent irradiations were conducted (Table 2). A thermal irradiation of highly enriched (93.13% ^{235}U) uranium (HEU) metal, sealed in a quartz ampule, was conducted at the Massachusetts Institute of Technology (MIT) Nuclear Reactor Laboratory for 200 minutes at 90 kW under a flux of 7.2 x 10^{10} n/cm^2/s to generate fission products. Five solid neutron activation targets sealed in LDPE vials were irradiated at the United States Geological Survey (USGS) TRIGA Reactor for 300 minutes in the Lazy Susan position at 1000 kW under a flux of 3.7 x 10^{12} n/cm^2/s. All targets were allowed to cool for approximately 48 h, then shipped to Los Alamos National Laboratory (LANL) for radiochemical analysis.

Each target was dissolved separately in individual beakers, then used to make solutions implemented in the validation experiments. All dissolutions were conducted using Fisher Scientific Optima Grade acids and 18 MΩ·cm water. The HEU foil was dissolved while heating using a mixture of 8 M HNO_3, 6 M HCl, and dilute HF.[42] Once dissolved, the solution was transposed to a 4 M HNO_3 matrix, then diluted to achieve a final concentration of 0.866 mg HEU·g^{-1} solution. Each activation product target was dissolved in a separate Pyrex beaker. The Au-Al wire was dissolved in aqua regia at room temperature. To the beaker containing the K_2IrCl_6/KCl powder, 0.5 M HCl was added at room temperature until the powder fully dissolved. The $CrCl_3 \cdot 6H_2O$ powder and the $H_2PtCl_6 \cdot xH_2O$ powder were each dissolved using H_2O at room temperature. The Ga_2Cl_4 was dissolved in 8 M HNO_3 at room temperature. The resultant HEU/fission product solution and each activation product solution were characterized individually via γ-spectroscopy to determine the activity of the fission products and activated isotopes, respectively. Each solution was also analyzed using ICP-OES to determine the elemental concentrations in each solution.

Following characterization of the HEU/fission product solution and each activation product solution, the sample used for validation experiments was prepared by combining aliquots of each the HEU/fission product, ^{198}Au, $^{192/194}$Ir, ^{72}Ga, ^{51}Cr, and $^{191/195m/197}$Pt solutions in an Erlenmeyer flask at the concentrations outlined in Table 2. Tracer solutions of ^{54}Mn, ^{57}Co, and ^{59}Fe, as well as an aliquot of SRM 2702 solution (10 mL, ~8.9 mg·g^{-1} solution), were also added. The activation product and fission product stable carrier solutions were then added in 5 mL and 2 mL portions,

respectively. At this stage, the activation product, fission product, and SRM mixture was converted to a 4 M HNO_3 matrix in preparation for separations.

Instrumentation and Sample Handling

Chemical yielding was conducted by ICP-OES using a ThermoFisher Scientific ICAP 6500 (Waltham, MA, USA) instrument fitted with an Elemental Scientific Inc. (ESI, Omaha, NE, USA) auto-sampler. The ICP-OES is fitted to a radiological fume hood to assist in preventing personnel contamination. An axial view of the ICP was employed for photon collection to achieve optimal sensitivity. An ESI Perfluoroalkoxy (PFA) low-flow nebulizer housed within a Teflon® cyclonic spray chamber was utilized. This instrument configuration for the analysis of radiological materials has been described previously.[43, 44] Calibration curves were developed for each element prior to each analysis using custom-made certified standard solutions from High-Purity Standards. All samples analyzed by ICP-OES were diluted as needed to fall within the concentration range of the calibration curves. The instrument was evaluated for reproducibility, stability, and instrument drift over a test in-run analysis (6 h length) as well as day-to-day measurements (over 60 d). No significant variations were observed in the timeframes evaluated, indicating that the impact of instrument drift is minimal even when long run times are required for sample analysis.

Calibrated high-purity Ge (HPGe) detectors with either an aluminum or beryllium window were used for γ-spectroscopy measurements. Certified multi-line standards containing emissions from 59 keV (^{241}Am) to 1836 keV (^{88}Y) were used to determine the efficiency of each detector and position for the specified sample geometry. All analytical samples were measured using the calibrated sample geometry.

Results and Discussion

The primary goal of this effort was to develop a method for rapidly isolating microscopic quantities (10^{-3} to 10^{-6} atoms per ^{235}U fission) of several activation products (^{198}Au, $^{192/194}Ir$, ^{72}Ga, ^{51}Cr, $^{191/195m/197}Pt$, ^{54}Mn, ^{57}Co, and ^{59}Fe) from soil matrixes contaminated with fresh fission products. Following the method development using stable carriers, the process was validated by conducting several experiments with fresh activation products and fission products. Representative details of the experiments are described herein. A general discussion of the activation product separation procedure follows.

Method Validation: Separation of Activation Products from Fission Products, Uranium, and Soil Matrix

Following the development of the separations protocol using stable carriers, several validation experiments were carried out using fresh activation products and fission products to test the effectiveness of the procedure for use in activation product qualitative analyses. Irradiation targets were prepared from ^{235}U metal and several stable materials (0.12% Au-Al wire, a K_2IrCl_6/KCl pellet, Ga_2Cl_4, $CrCl_3 \cdot 6H_2O$, and $H_2PtCl_6 \cdot xH_2O$). Fresh fission products and short-lived neutron activation products (^{51}Cr, ^{72}Ga, $^{192/194}Ir$, $^{191/195m/197}Pt$, and ^{198}Au) were produced at the Massachusetts Institute of Technology Nuclear Research Reactor and at the United States Geological Survey (USGS) Training, Isotopes, and General Atomics (TRIGA) Reactor, respectively. The targets were then returned to LANL, dissolved, and characterized. Tracer solutions of ^{54}Mn, ^{57}Co, and ^{59}Fe were purchased from Eckert and Ziegler and used as received.

The individual solutions were subsequently combined to prepare the experimental sample solution employed in the experiments used for separations validation. This involved combining aliquots of each the HEU/fission product, ^{198}Au, $^{192/194}$Ir, ^{72}Ga, ^{51}Cr, $^{191/195m/197}$Pt, ^{54}Mn, ^{57}Co, and ^{59}Fe solutions to achieve activation product quantities that ranged from 10^{-3} to 10^{-6} atoms per ^{235}U fission. To simulate environmental samples – those that contain soil matrix and chemical interferences from the environment – the fission product and activation product cocktail was combined with an aliquot of SRM 2702 solution (containing ~89 mg of soil). Our activation product processing method relies on the addition of macroscopic amounts of stable elements, on the order of 0.2 mg for the stable fission product elements (Ba, Ce, La, Mo, Nd, Sr, Te, Y, and Zr) and 1 mg for the stable activation product elements (Au, Co, Cr, Cu, Fe, Ga, Ir, Mn, Ni, Pb (5 mg), Pb, Pt, Sc, and Zn) product elements. Having analytes present in these large quantities ensures that the isotopes adopt predictable behavior associated with a bulk sample. In addition, it provides potential opportunity to determine separation yields gravimetrically.

After adding the stable carriers to the sample (the solution containing soil matrix, fission products, uranium, and the desired activation products), the aqueous matrix was converted to HNO_3 (4 M) with a final volume of 10 mL. The solution was then processed as summarized in Fig. 2. The first step in the procedure was developed to isolate a tungsten fraction (W). This was achieved by precipitation of W with 1 mL of a W carrier (10,000 $\mu g \cdot mL^{-1}$ in water, SpexCertiPrep).[45–49] Quantitative removal of W from the stock solution made it impossible to determine a decontamination factor. Subsequently, Pb was removed by a similar precipitation using Pb carrier (0.5 mL; 10,000 $\mu g \cdot mL^{-1}$ in 5% HNO_3; Spex CertiPrep).[49] Typically, Pb decontamination factors for this separation step were near quantitative, with the Pb recoveries

often near 100%. However, this step is not robust and at times Pb yields can be as low as 5%. When Pb yields are low from the precipitation step, screening can still occur using the AGMP-1M chromatographic step described below. Although it is tempting to eliminate the Pb precipitation, we recommend retaining this separation step. It is valuable because several fission products (Ce, 80%; Mo, 20%; Te, 10%; and U 30%) co-precipitate with the W and Pb carriers, which facilitates the subsequent screening effort.[46]

After removing W and Pb, the sample was converted to 6 M HCl matrix and subjected to ion exchange chromatography. A moderately sized column (Bio-Rad, with 25 mL of AGMP-1M resin) was used to accommodate the large variability in analyte distribution constants. To ensure rapid separation for this step (within 90 min), sample processing was integrated with high performance liquid chromatographic (HPLC) methodology (flow rate = 5 $mL \cdot min^{-1}$). Given the high corrosivity of the eluents, special consideration was made to employ a pump with acid-resistant components. After loading the sample onto the column in HCl (6 M), a step-wise gradient elution was conducted from HCl (6 M) to H_2O, and then to thiourea (7%, w/w). As described in Fig. 3, this approach results in six main cuts that were collected in thirty-seven individual fractions (10 mL each). The first cut (Cut I) contained Pb and Co, with smaller quantities of Sc, Ir, Ni, Cu, Cr, Ga, and Mn. Cut II contains primarily Cu and a sufficient amount of Ir for qualitative evaluation by gamma spectroscopy. Cut III was isolated by first stepping the HCl concentration down from 6 M to 4 M and then stepping down again to 2 M. This fraction contained appreciable amounts of Au and Ga, with small quantities of Pt and Ir also present. Iron was also able to be detected by γ-spectroscopy, despite the poor chemical recovery in the Ga/Fe cut (Cut III), as indicated in Table 3.[2] Changing

[2] In the presence of soil matrix, Fe recoveries are not reproducible. In the absence of soil matrix, Fe recoveries were determined by ICP-OES to be near quantitative.

the mobile phase to water (H_2O), Cut IV containing only Zn eluted. To elute Au and Pt, the mobile phase was changed to thiourea. In dilute thiourea (1%) Au and some Pt eluted in Cut V. In more concentrated thiourea (7%), Pt is fully removed in Cut VI, which also contained small amounts of Au and Ir. Typical decontamination factors and percent recoveries for each element are shown in Table 1.

Following the chromatography step with AGMP-1M, separated fractions were characterized by ICP-OES and γ-spectroscopy. In general, fission products were removed to the point that they did not interfere with the activation product analyses. Exceptions to this generality were associated with the ^{194}Ir, ^{54}Mn, and ^{51}Cr analytes. The gamma spectrum from the Ir/Cu cut had significant contributions from ^{140}La (328.76 keV), which interfered with ^{194}Ir detection. Fission products that also eluted in the ^{54}Mn/^{51}Cr/Sc/Ni fraction contributed to a high background preventing these two activation products from being accurately detected. Another issue was associated with the Au and Pt recoveries, which were significantly greater than 100%. This discrepancy resulted from challenges associated with accurately accounting for precipitation of stable Au and Pt carriers in the activation product carrier solution used for yield quantification.[50, 51]

Following γ-spectroscopy measurements and chemical yielding determination for the first three fractions from the AGMP-1M separation, the fractions were combined and subjected to additional chromatography to further resolve ^{54}Mn and ^{51}Cr from the fission product interferences. The combined fractions underwent an additional chromatography step using a 20 mL column filled with the commercially available DGA resin (3 mL). This added step was attractive because it enabled pure fractions of ^{51}Cr/Ni, ^{54}Mn, and Sc to be isolated from main group, lanthanide, and

transition metal fission product interferences (e.g. Ba, La, Ce, Sr, Nd, Y, Zr). Moreover, it could be completed rapidly (only adding 1 hour to the entire process). As represented in Fig. 4, the sample was loaded in HCl (6 M) onto the column and subjected to a four-step gradient elution profile: first HCl (6 M), then HCl (4 M), HCl (2 M), and finally H_2O. Pressure was added to the column using the in-house air line until a flow rate of approximately 1 drop per second was reached. Samples were collected in nine total fractions (5 mL each). Chromium and Ni eluted during step one (HCl, 6 M) in the first two fractions. During the first elution step (still HCl, 6 M), Mn began eluting in fraction 2. To elute Mn from the column in the smallest possible volume, the HCl concentration was decreased to 4 M in step two of the gradient elution, which caused the majority of Mn to elute in fractions 3 and 4. The mobile phase was changed to 2 M (step three) after Mn finished eluting. This change caused Sc to begin eluting from the column in fraction 7. The mobile phase was then switched to H_2O (step four) and Sc was completely recovered. To determine decontamination factors and chemical yields, the resultant Cr/Ni, Mn, and Sc fractions were analyzed by ICP-OES (Table 1).

Outlook and Conclusion

Contributed here is an HPLC-based processing method that rapidly removes activation products from fission products, uranium, and contaminants associated with soil matrixes. Activation product identities are qualitatively characterized using γ-spectroscopy and elemental abundances quantified by ICP-OES. Although additional research is needed to demonstrate generality, the hallmark of this study is proof-of-principle. As a testament, the procedure was validated for ^{198}Au, ^{192}Ir, ^{72}Ga, ^{51}Cr, $^{191/195m/197}$Pt, ^{54}Mn, ^{57}Co, and ^{59}Fe.

The simplicity of the procedure is attractive; the process can be carried out by researchers with a wide range of technical expertise. Broad operator access should facilitate implementation into a wide range of scientific laboratories and provide potential support for numerous scientific campaigns with diverse mission scope. Consider the importance of characterizing a nuclear fission event by identifying the presence (or absence) of a given activation product. This qualitative screen could serve as a diagnostic to guide subsequent experimental efforts. In addition, the procedure could be used as a crude separation step that precedes further sample processing and quantification efforts. We hope the process will find applicability in characterizing the impact of activation products emitted from nuclear contamination sites and inspire researchers to identify nuclear signatures and define inter-element ratios for non-actinide activation products.

Acknowledgements

The authors are grateful for support from the Defense Threat Reduction Agency.

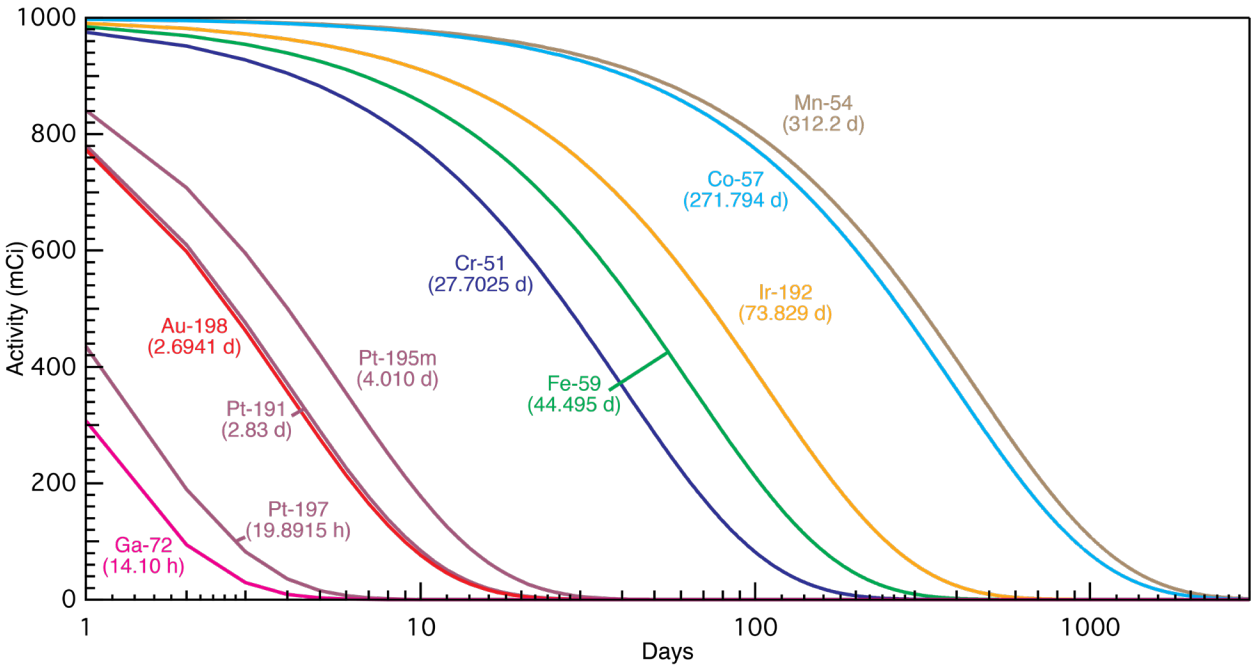

Figure 1. Activation product activity plotted as a function of increasing time from production.

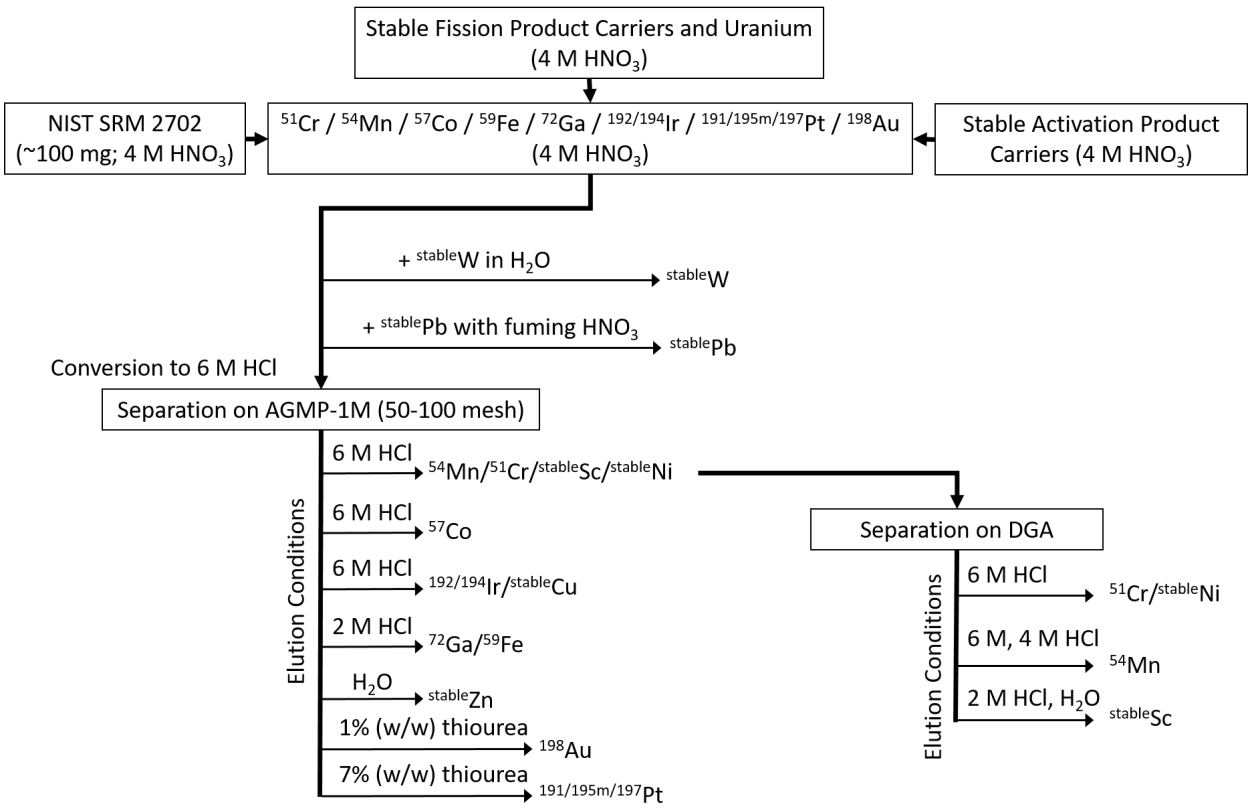

Figure 2. Separation scheme for isolation of activation products in this study

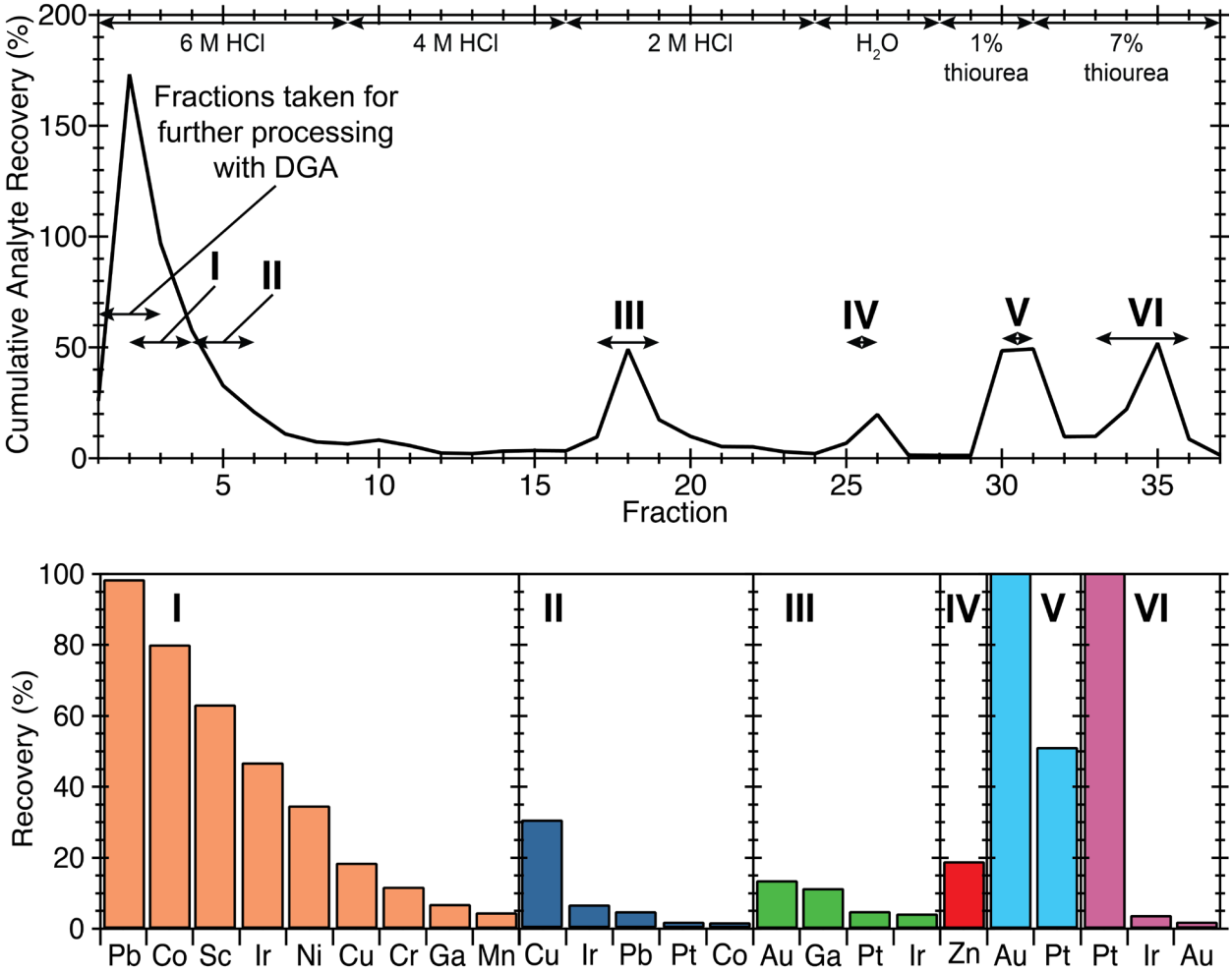

Figure 3. Percent recovery of activation products from AGMP-1M separation, with the chromatographic fraction vs the cumulative analyte recovery shown on the top. Along the bottom, from left to right, are the individual cuts for Pb/Co (I), Ir/Cu (II), Ga/Fe (III), Zn (IV), Au (V), and Pt (VI). Illustrated for each cut are the activation products that also co-elute.

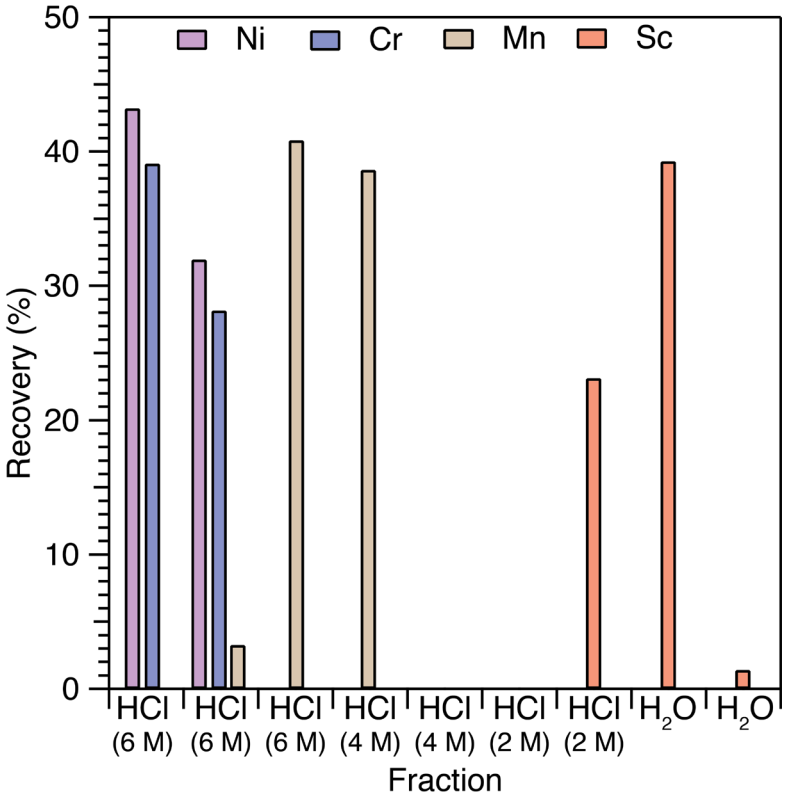

Figure 4. Percent recovery of Cr, Ni, Mn, and Sc from DGA separation with the combined first three fractions from AGMP-1M separation, per individual fraction.

Table 1. Typical Overall Percent Recoveries and Decontamination Factors of Activation Products

Element	**Percent Recovery (ICP-OES)**	**Decontamination Factor**
Au	92.4	13.2
Co	85.5	6.9
Cr	3.1	1.0
Cu	90.2	10.2
Fe	74.6	3.9
Ga	96.0	25
Ir[a]	57.1	2.3
Mn	1.3	1.0
Ni	10.6	1.1
Pb	74.4	3.9
Pt	97.4	38.4
Sc	4.2	1.0
W	>100	N/A[b]
Zn	19.6	1.2

[a] Percent recoveries of Ir varied greatly and were not reproducible.
[b] Decontamination factor unable to be determined due to complete removal during precipitation step; no W was detected in any of the separated fractions.

Table 2. Typical materials used in validation experiments

Target Material	Nuclear Reaction(s) of Interest	Irradiation Location	Target Mass (mg)	Irradiated Target Concentration Added to Validation Sample Matrix[a]
93.13% ^{235}U foil[b]	(n,f)	MIT	62.6	8.81E+12 fissions[c]
0.12% Au-Al wire	^{197}Au(n,γ)^{198}Au	USGS	0.10 (Au) 86.6 (total)	3.90E-04 N ^{198}Au/fission
K_2IrCl_6/KCl	^{191}Ir(n,γ)^{192}Ir ^{193}Ir(n,γ)^{194}Ir	USGS	0.56 (K_2IrCl_6) 6.06 (total)	1.58E-02 N ^{192}Ir/fission
Ga_2Cl_4	^{71}Ga(n,γ)^{72}Ga	USGS	124.9	7.59E-06 N ^{72}Ga/fission
$CrCl_3 \cdot 6H_2O$	^{50}Cr(n,γ)^{51}Cr	USGS	104.5	1.52E-03 N ^{51}Cr/fission
$H_2PtCl_6 \cdot xH_2O$	^{190}Pt(n,γ)^{191}Pt ^{194}Pt(n,γ)^{195m}Pt ^{196}Pt(n,γ)^{197}Pt	USGS	499.2	3.42E-05 N ^{191}Pt/fission 1.96E-04 N ^{195m}Pt/fission 2.04E-05 N ^{197}Pt/fission
^{54}Mn tracer[d]	n/a	n/a	n/a	1.54E-03 N ^{54}Mn/fission
^{57}Co tracer[d]	n/a	n/a	n/a	1.49E-03 N ^{57}Co/fission
^{59}Fe tracer[d]	n/a	n/a	n/a	9.48E-04 N ^{59}Fe/fission

[a] Activation product concentrations are reported as number of atoms per ^{235}U fission.
[b] The ^{235}U metal was pickled to remove any surface oxide, then dried before being sealed in a quartz ampule for irradiation.
[c] Fissions were determined using gamma-counting analysis of ^{99}Mo from the ^{235}U solution.
[d] Tracers were purchased from Eckert & Ziegler and used as received.

Table 3. Activation Product Results from Each Cut in the Validation Experiment

Cut	Element	Percent Recovered by ICP-OES[a,b,c]	Percent Uncertainty in ICP-OES Measurement (k = 2)
Cr/Ni	Cr	9.1	0.19
	Ni	31.8	0.18
Mn	Mn	4.0	0.27
Sc	Sc	49.0	0.20
Pb/Co	Co	80.2	0.42
	Cr	11.9	0.19
	Cu	18.7	0.44
	Ga	7.1	0.36
	Ir	46.8	0.28
	Mn	4.7	0.27
	Ni	34.8	0.18
	Pb	98.6	4.5
	Sc	63.2	0.20
Ir/Cu	Co	1.7	0.42
	Cu	30.6	0.44
	Ir	6.7	0.28
	Pb	4.8	4.5
	Pt	1.8	1.21
Ga/Fe	Au	13.7	0.23
	Fe	nd[d]	--
	Ga	11.6	0.36
	Ir	4.3	0.28
	Pt	5.1	1.21
Zn	Zn	18.4	0.41
Au	Au	>>100	0.23
	Pt	51.2	1.21
Pt	Au	2.0	0.23
	Ir	3.9	0.28
	Pt	>>100	1.21

[a] Values for Au and Pt are >100% due to precipitation of those elements from the ingoing activation product stable carrier solution. From this result, it was determined that the activation product stable carrier solution shelf-life is ~18 months.
[b] Determined from stable target mass added.
[c] The chemical yield accounts for stable target mass or contributions from SRM 2702 in the experimental load solution.
[d] nd – not detected

References

1. Horan JR (1963) The health physics aspects of the SL-1 accident. Health Phys 9:177–186
2. Mitsugashira T, Hara M, Nakanishi T, et al (2000) Passive gamma-ray spectrometry for the determination of total fission events in the JCO criticality accident '99 in Tokai. J Environ Radioact 50:21–26. https://doi.org/10.1016/S0265-931X(00)00056-4
3. Tanaka S-I (2001) Summary of the JCO Criticality Accident in Tokai-mura and a Dose Assessment. J Radiat Res 42:S1–S9. https://doi.org/10.1269/jrr.42.S1
4. Selby JM, Moeller DW, Vallario EJ, Stephan JG (1986) Use of Radiological Accident Experience in Establishing Appropriate Perspectives in Emergency Planning. In: ANS Topical Meeting on Radiological Accidents - Perspectives and Emergency Planning. Bethesda
5. McLaughlin TP, Monahan SP, Pruvost NL, et al (2000) A Review of Criticality Accidents. Los Alamos
6. Inaba J (2000) Radiological and Environmental Aspects of the Criticality Accident in Tokai-mura. Radiat Prot Dosimetry 92:239–246. https://doi.org/10.1093/oxfordjournals.rpd.a033277
7. Napier BA, Schmieman EA, Voitsekovitch O (2007) RADIOACTIVE WASTE MANAGEMENT AND ENVIRONMENTAL CONTAMINATION ISSUES AT THE CHERNOBYL SITE. Health Phys 93:441–451. https://doi.org/10.1097/01.HP.0000279602.34009.e3
8. Podlazov LN, Trekhov VE, Cherkashov YM, et al (1994) Computational modeling of the accident in the fourth power-generating unit of the chernobyl nuclear power plant. At Energy 77:580–587. https://doi.org/10.1007/BF02407430
9. Kofuji H, Komura K, Yamada Y, Yamamoto M (2000) An estimation of fast neutron flux by reaction. J Environ Radioact 50:49–54. https://doi.org/10.1016/S0265-931X(00)00060-6
10. Muroyama T, Murata Y, Kofuji H, et al (2000) Neutron activation of chemical reagents exposed to the neutrons released by the JCO criticality accident. J Environ Radioact 50:55–59. https://doi.org/10.1016/S0265-931X(00)00061-8
11. Imanaka T (2000) Neutron dose and power released by the JCO criticality accident in Tokai-mura. J Environ Radioact 50:15–20. https://doi.org/10.1016/S0265-931X(00)00055-2
12. Furuta K, Sasou K, Kubota R, et al (2000) Human Factor Analysis of JCO Criticality Accident. Cogn Technol Work 2:182–203. https://doi.org/10.1007/PL00011501
13. Komura K, Yamamoto M, Muroyama T, et al (2000) The JCO criticality accident at Tokai-mura, Japan: an overview of the sampling campaign and preliminary results. J Environ Radioact 50:3–14. https://doi.org/10.1016/S0265-931X(00)00054-0
14. Komura K, Yousef AM, Murata Y, et al (2000) Activation of gold by the neutrons from the JCO accident. J Environ Radioact 50:77–82. https://doi.org/10.1016/S0265-931X(00)00064-3
15. Takada J, Hoshi M (2000) External doses to 350m zone residents around the Tokai-mura criticality accident site. J Environ Radioact 50:43–48. https://doi.org/10.1016/S0265-931X(00)00059-X
16. Imanaka T (2001) Transport Calculation of Neutrons Leaked to the Surroundings of the Facilities by the JCO Criticality Accident in Tokai-mura. J Radiat Res 42:S31–S44.

https://doi.org/10.1269/jrr.42.S31
17. Evans JC, Lepel EL, Sanders RW, et al (1984) Long-lived activation products in reactor materials. Richland
18. Buesseler K, Aoyama M, Fukasawa M (2011) Impacts of the Fukushima Nuclear Power Plants on Marine Radioactivity. Environ Sci Technol 45:9931–9935. https://doi.org/10.1021/es202816c
19. Shozugawa K, Nogawa N, Matsuo M (2012) Deposition of fission and activation products after the Fukushima Dai-ichi nuclear power plant accident. Environ Pollut 163:243–247. https://doi.org/10.1016/j.envpol.2012.01.001
20. Schwantes JM, Orton CR, Clark RA (2012) Analysis of a Nuclear Accident: Fission and Activation Product Releases from the Fukushima Daiichi Nuclear Facility as Remote Indicators of Source Identification, Extent of Release, and State of Damaged Spent Nuclear Fuel. Environ Sci Technol 46:8621–8627. https://doi.org/10.1021/es300556m
21. Mattsson S, Finck R, Nilsson M (1980) Distribution of activation products from barsebäck nuclear power plant (Sweden) in the marine environment. Temporal and spatial variations as established by seaweed. Environ Pollut Ser B, Chem Phys 1:105–115. https://doi.org/10.1016/0143-148X(80)90031-2
22. Le Petit G, Douysset G, Ducros G, et al (2014) Analysis of Radionuclide Releases from the Fukushima Dai-Ichi Nuclear Power Plant Accident Part I. Pure Appl Geophys 171:629–644. https://doi.org/10.1007/s00024-012-0581-6
23. Achim P, Monfort M, Le Petit G, et al (2014) Analysis of Radionuclide Releases from the Fukushima Dai-ichi Nuclear Power Plant Accident Part II. Pure Appl Geophys 171:645–667. https://doi.org/10.1007/s00024-012-0578-1
24. Donaldson LR, Seymour AH, Nevissi AE (1997) University of Washington's Radioecological Studies in the Marshall Islands, 1946–1977. Health Phys 73:214–222. https://doi.org/10.1097/00004032-199707000-00018
25. Oughton DH, Day JP (1993) Determination of cesium, rubidium and scandium in biological and environmental materials by neutron activation analysis. J Radioanal Nucl Chem Artic 174:177–185. https://doi.org/10.1007/BF02040345
26. Inaba J (2015) Environmental Transfer Parameters of Radionuclides. Radioisotopes 64:335–349. https://doi.org/10.3769/radioisotopes.64.335
27. Warren GA, Runkle RC (2013) New concepts for radiometric measurements of environmental samples. J Radioanal Nucl Chem 296:829–833. https://doi.org/10.1007/s10967-012-2133-z
28. Winkler SR, Steier P, Carilli J (2012) Bomb fall-out 236U as a global oceanic tracer using an annually resolved coral core. Earth Planet Sci Lett 359–360:124–130. https://doi.org/10.1016/j.epsl.2012.10.004
29. Froehlich MB, Tims SG, Fallon SJ, et al (2017) Nuclear weapons produced 236 U, 239 Pu and 240 Pu archived in a Porites Lutea coral from Enewetak Atoll. J Environ Radioact 178–179:349–353. https://doi.org/10.1016/j.jenvrad.2017.05.009
30. De Cesare M, De Cesare N, D'Onofrio A, et al (2015) Mass and abundance 236 U sensitivities at CIRCE. Nucl Instruments Methods Phys Res Sect B Beam Interact with Mater Atoms 361:483–487. https://doi.org/10.1016/j.nimb.2015.05.029
31. De Cesare M, Gialanella L, Rogalla D, et al (2010) Actinides AMS at CIRCE in Caserta (Italy). Nucl Instruments Methods Phys Res Sect B Beam Interact with Mater Atoms 268:779–783. https://doi.org/10.1016/j.nimb.2009.10.029

32. Mahara Y, Kudo A (1995) Plutonium released by the Nagasaki A-bomb: Mobility in the environment. Appl Radiat Isot 46:1191–1201. https://doi.org/10.1016/0969-8043(95)00161-6
33. Yuanzhong L, Jianzhu C (2002) Fission product release and its environment impact for normal reactor operations and for relevant accidents. Nucl Eng Des 218:81–90. https://doi.org/10.1016/S0029-5493(02)00200-5
34. Tadmor J (1976) Determination of the Type and Amount of Fission Products Released in a Nuclear Reactor Accident. Health Phys 30:95–112. https://doi.org/10.1097/00004032-197601000-00011
35. Hanson SK, Pollington AD, Waidmann CR, et al (2016) Measurements of extinct fission products in nuclear bomb debris: Determination of the yield of the Trinity nuclear test 70 y later. Proc Natl Acad Sci 113:8104–8108. https://doi.org/10.1073/pnas.1602792113
36. Goldstein SJ, Hinrichs KA, Nunn AJ, et al (2018) Sequential chemical separations and multiple ion counting ICP-MS for 241Pu–241Am–237Np dating of environmental collections on a single aliquot. J Radioanal Nucl Chem 318:695–701. https://doi.org/10.1073/pnas.1602792113
37. Biegalski SR, Bowyer TW, Eslinger PW, et al (2012) Analysis of data from sensitive U.S. monitoring stations for the Fukushima Dai-ichi nuclear reactor accident. J Environ Radioact 114:15–21. https://doi.org/10.1016/j.jenvrad.2011.11.007
38. Thakur P, Ballard S, Nelson R (2013) An overview of Fukushima radionuclides measured in the northern hemisphere. Sci Total Environ 458–460:577–613. https://doi.org/10.1016/j.scitotenv.2013.03.105
39. Quinto F, Golser R, Lagos M, et al (2015) Accelerator Mass Spectrometry of Actinides in Ground- and Seawater: An Innovative Method Allowing for the Simultaneous Analysis of U, Np, Pu, Am, and Cm Isotopes below ppq Levels. Anal Chem 87:5766–5773. https://doi.org/10.1021/acs.analchem.5b00980
40. Morrison SS (2015) Activation Product Analysis in the Presence of Fission Products. Washington State University
41. Kleinberg J (1990) Collected Radiochemical and Geochemical Procedures
42. Laue CA, Gates-Anderson D, Fitch TE (2004) Dissolution of metallic uranium and its alloys. J Radioanal Nucl Chem 261:709–717. https://doi.org/10.1023/B:JRNC.0000037117.01721.f1
43. Gao J, Manard BT, Castro A, et al (2017) Solid-phase extraction microfluidic devices for matrix removal in trace element assay of actinide materials. Talanta 167:8–13. https://doi.org/10.1016/j.talanta.2017.01.080
44. Montoya DP, Manard BT, Xu N (2016) Novel sample introduction system to reduce ICP-OES sample size for plutonium metal trace impurity determination. J Radioanal Nucl Chem 307:2009–2014. https://doi.org/10.1007/s10967-015-4648-6
45. Korob RO, Cohen IM, Agatiello OE (1976) Tungsten and molybdenum co-precipitation by α-benzoinoxime for activation analysis of tungsten. J Radioanal Chem 34:329–333. https://doi.org/10.1007/BF02519582
46. Knowles HB (1932) The use of alpha-benzoinoxime in the determination of molybdenum. Bur Stand J Res 9:1–8. https://doi.org/10.1016/S0016-0032(13)90386-0
47. Yagoda H, Fales HA (1938) Studies on the Analytical Chemistry of Tungsten and Molybdenum. II. J Am Chem Soc 60:640–643. https://doi.org/10.1021/ja01270a041
48. Taylor-Austin E (1937) The Determination of Molybdenum in Cast Iron. Analyst 107–117

49. Unknown Authors (1971) Separation of a Mixture of the Elements MCL-LP-06-04. Los Alamos
50. Borgarello E, Serpone N, Emo G, et al (1986) Light-induced reduction of rhodium(III) and palladium(II) on titanium dioxide dispersions and the selective photochemical separation and recovery of gold(III), platinum(IV), and rhodium(III) in chloride media. Inorg Chem 25:4499–4503. https://doi.org/10.1021/ic00245a010
51. Torigoe K, Esumi K (1992) Preparation of colloidal gold by photoreduction of tetracyanoaurate(1-)-cationic surfactant complexes. Langmuir 8:59–63. https://doi.org/10.1021/la00037a013